Physicochemical and functional properties of extruded wheat bran dietary fiber: Effects on slow transit constipation

Zhan Wang[1,2], Dong Tan[1], Kemeng Zhao[1], Wangyang Shen[1,2], Xiwu Jia[1,2]*, Bo Liu[3]*

[1]School of Food Science and Engineering, Wuhan Polytechnic University, Wuhan, China; [2]Key Laboratory for Deep Processing of Major Grain and Oil, Ministry of Education, Wuhan, China; [3]Faculty of Pharmacy, Hubei University of Chinese Medicine, Wuhan, China

***Corresponding Authors**: Xiwu Jia, School of Food Science and Engineering, Wuhan Polytechnic University, Wuhan, China. Email: jiaxiwu212@126.com; Bo Liu, Faculty of Pharmacy, Hubei University of Chinese Medicine, Wuhan, China. Email: 4860715@qq.com

Academic Editor: Prof. Valeria Sileoni – Universitas Mercatorum, Italy

Received: 26 September 2024: Accepted: 17 December 2024; Published: 8 January 2025

ORIGINAL ARTICLE

Abstract

This study investigated wheat bran dietary fiber (WBDF) using the twin-screw extrusion method, with wheat bran as the primary raw material. The research examined the physicochemical properties, cholesterol and sodium cholate adsorption capacity, thermogravimetric analysis, X-ray diffraction, and functional characteristics. Animal experiments were conducted to assess its impact on improving constipation. Results indicated that extrusion-modified WBDF (E-WBDF) exhibited higher water-holding capacity (WHC), oil-holding capacity (OHC), water swelling capacity (WSC), and stronger cholesterol and sodium cholate adsorption capacities (CAC and SCAC). Additionally, E-WBDF showed greater DPPH and ABTS scavenging activities compared to WBDF. In mouse models of slow transit constipation, both WBDF and E-WBDF significantly alleviated constipation, with E-WBDF demonstrating superior efficacy. These findings highlight that E-WBDF could serve as a promising functional food additive to enhance intestinal function.

Keywords: constipation; extrusion; functional characteristics; wheat bran dietary fiber

Introduction

Wheat is a fundamental staple in global diets, providing a significant portion of daily energy, fiber, and essential micronutrients (Brouns *et al*., 2019). Wheat bran (WB), which constitutes approximately 25% of the weight of milled wheat, is the outer fibrous layer of the wheat grain. It is rich in dietary fiber (DF), proteins, vitamins, and minerals (Prückler *et al*., 2014), offering notable nutritional and health benefits. WB is obtained through conventional grain milling processes involving dissociation and separation technologies, along with starchy endosperm (flour) extraction. With a total DF (TDF) content typically exceeding 50% of its total weight, WB is primarily composed of insoluble DF (IDF), which accounts for over 90% of its TDF content (Cheng *et al*., 2022). DF includes plant-derived or analogous carbohydrates that resist digestion and absorption in the human small intestine, undergoing partial or complete fermentation in the large intestine (DeVries, 2003). Consumption of wheat bran dietary fiber (WBDF) significantly contributes to alleviating constipation (Maffei & Vicentini, 2011). Furthermore, DF shows promising potential in the prevention and management of various conditions,

including but not limited to diabetes, obesity, cardiovascular disease, gastrointestinal disorders, and colorectal cancer (Threapleton *et al*., 2013; Oh *et al*., 2019; Solah *et al*., 2017).

Currently, the primary use of bran is in animal feed due to its numerous physiological benefits, particularly in promoting gastrointestinal health. However, its high DF content limits its incorporation into human food products, as it can negatively affect their quality characteristics. Directly adding WB to food processing can compromise product quality. Therefore, selecting an appropriate treatment method to enhance the value of WB is crucial. Various modification methods exist, including alkaline hydrogen peroxide treatment, microwave extraction, enzymatic hydrolysis, extrusion, steam explosion, and ultrasonic-assisted extraction (Liu *et al*., 2021; Sui *et al*., 2018; Ye *et al*., 2021). Extrusion technology, which offers numerous advantages over other processing methods, has rapidly transformed the food industry. It enables continuous and automated processing, allowing precise control of parameters such as temperature, pressure, and residence time, resulting in efficient production with consistent product quality. Ramos-Enríquez *et al*. found that extrusion significantly increased the content of bound phenolic compounds and antioxidant capacity in extruded WB (EWB) (Ramos-Enríquez *et al*., 2018). Additionally, Ye *et al*. reported that extrusion of WB can enhance the content and digestibility of soluble DF while extending product shelf life (Ye *et al*., 2021). Zhang *et al*. also demonstrated that modifying WB using extrusion and semisolid enzymatic hydrolysis with xylanase improves the processing and edible quality of bran-containing flour products (Zhang *et al*., 2022). Incorporating extrusion as a pretreatment for composite feedstock containing cereal or legume by-products may limit molecular modifications, thereby enhancing nutritional properties. This approach presents an interesting and economical alternative to improving the nutrient profile and bioavailability of cereal and legume by-products, potentially leading to the development of functional ingredients for producing foods aimed at preventing chronic diseases (Orozco-Angelino *et al*., 2023).

Constipation, a prevalent digestive disorder, is becoming increasingly common due to modern lifestyle and dietary changes, significantly impacting people's quality of life. It is characterized by difficulties in defecation, infrequent bowel movements, dry and hard stools, and prolonged gastrointestinal transit time (Bharucha, 2007). Previous studies indicate that DF plays a role in preventing chronic diseases such as obesity, colorectal cancer, and diabetes by regulating intestinal flora (Barber *et al*., 2020). DF shows promise as a safe dietary supplement with minimal side effects for managing both chronic and occasional constipation in humans (Ma *et al*., 2023). Moreover, by increasing fecal volume and water content, DF can stimulate intestinal peristalsis and alleviate constipation symptoms (Lai *et al*., 2023). Studies have demonstrated that IDF notably influences mouse fecal water content in a dose-dependent manner, suggesting its laxative effects (Cao *et al*., 2023).

This study compares the functional and physicochemical properties of WBDF before and after extrusion modification, including WHC, OHC, water swelling capacity (WSC), CAC, and SCAC. It investigates the impact of extrusion modification on the functional properties of WBDF and examines its potential to alleviate constipation by assessing parameters such as fecal volume, fecal water content, defecation time, small intestine transit rate, and more. These findings aim to provide a theoretical foundation for the enhanced utilization of WBDF and the development of functional products.

Material and Methods

Materials and reagents

WB was sourced from COFCO Flour (Wuhan) Co., Ltd. (Wuhan, China). Cholesterol standard, sodium cholate, phthalaldehyde, and loperamide hydrochloride were obtained from Shanghai Yuanye Biotechnology Co., Ltd. (Shanghai, China). Acetic acid and hydrochloric acid were procured from Shanghai Hushi Laboratorial Equipment Co., Ltd. (Shanghai, China). DPPH was acquired from TCI Shanghai (Shanghai, China). APTS was purchased from Wuhan Feiyang Biotechnology Co., Ltd. (Wuhan, China). Male Kunming mice (aged 6–8 weeks) were obtained from the Hubei Province Center for Disease Control and Prevention. Sterile saline was sourced from Sichuan Kelun Pharmaceutical Co., Ltd. (Sichuan, China). Indian Ink was purchased from Beijing Regen Biotechnology Co., Ltd. (Beijing, China).

Preparation of E-WBDF

Extrusion experiments were conducted using a corotating twin-screw extruder (model FMHE3-24; Hunan Fumach Foodstuff Engineering & Technology Co., Ltd., Hunan, China). The extrusion process involved setting temperatures at 60°C, 90°C, 120°C, 140°C, and 130°C for Zones II, III, IV, V, and VI, respectively. Based on preliminary investigations, a feeding speed of 17 kg/h and a screw speed of 160 r/min were selected (Zhang *et al*., 2022). The resulting E-WBDF was produced by eliminating phytic acid, fat, starch, protein, and other constituents, as detailed in previous studies.

Water-/oil-holding capacity (WHC/OHC) and WSC evaluation

The WHC and OHC were assessed following the method outlined by Nawrocka and Sangnark, with

minor adjustments (Nawrocka *et al*., 2017; Sangnark & Noomhorm, 2003). Dry samples were mixed with distilled water (1:20, w/v) for 12 h and with soybean oil (1:20, w/v) for 12 h in centrifuge tubes at room temperature. Subsequently, the mixtures were centrifuged at 4000 r/min for 20 min each. The WHC and OHC were then calculated using the following formulas:

$$\mathrm{WHC(g/g)} = \frac{M_2 - M_0}{M_1} \quad (1)$$

where M_0 represents the initial weight of the centrifuge tube (g), M_1 is the weight of the dried sample (g), and W_2 is the weight of the hydrated sample (g).

$$\mathrm{ORC(g/g)} = \frac{M_5 - M_4}{M_3} \quad (2)$$

where M_4 indicates the initial weight of the centrifuge (g), M_3 is the weight of the dried sample (g), and W_5 represents the weight of the hydrated sample (g).

The WSC was evaluated using a method adapted from Wang with minor adjustments (Wang *et al*., 2012). A precisely weighed dry sample (1.0 g) was gradually combined with 20 mL of distilled water in a measuring cylinder. The mixture was allowed to hydrate for 12 h at room temperature. The volumes of the solid and hydrated samples were then recorded.

$$\mathrm{WSC(ml/g)} = \frac{V_1 - V_2}{M} \quad (3)$$

where M represents the weight of the dried sample (g), V_1 is the volume of the dried sample (mL), and V_2 is the volume of the hydrated sample (mL).

Cholesterol and sodium cholate adsorption capacity (CAC and SCAC) evaluation

CAC and SCAC were determined following the method outlined by Wang and Kahlon with minor modifications (Wang *et al*., 2012; Kahlon *et al*., 2004). CAC was assessed using the o-phthalaldehyde method, and the absorbance of samples at 550 nm was measured using a spectrophotometer (UV-1800PC, Shanghai, China). Cholesterol content was quantified based on a standard curve (y = 0.0019x + 0.0026, R^2 = 0.9976). SCAC was determined using the furfural colorimetric method, with absorbance readings at 730 nm measured using the same spectrophotometer. Sodium cholate content was quantified using a standard curve (y = 1.3559x – 0.0241, R^2 = 0.99). The CAC and SCAC were calculated using the following formulas:

$$\mathrm{CAC(mg/g)} = \left[\frac{N_1 - N_0}{M}\right] \quad (4)$$

where M represents the sample weight (g), N_0 is the cholesterol content of the egg yolk liquid after adsorption (mg), and N_1 is the cholesterol content of the egg yolk liquid before adsorption (mg).

$$\mathrm{SCAC(mg/g)} = \left[\frac{W_1 - W_3}{W_2}\right] \quad (5)$$

where W_2 represents the sample weight (g), W_1 is the sodium cholate content before adsorption (mg), and W3 is the sodium cholate content after adsorption (g).

Thermogravimetric analysis (TGA)

TGA was conducted using a thermal gravimetric analyzer (METTLER TOLEDO, Zurich, Switzerland) to assess the thermal stability of the WBDF. The samples were heated from 30°C to 800°C at a linear heating rate of 10°C/min.

X-ray diffraction (XRD) analysis

The WBDF samples were measured using an X-ray polycrystal diffractometer (D8 Advance, Bruker AXS, Germany). This analysis was conducted at room temperature utilizing a Cu–Kα radiation source (λ = 0.154 nm) with a step size of 0.02°. A scanning rate of 2°/min within the scattering range (2θ) of 5°–60° was employed. The crystallinity indexes of the samples were calculated according to the Segal method (Segal *et al*., 1959).

Antioxidant activity

The DPPH scavenging capacity of WBDF was evaluated following the method outlined by Yan with minor modifications (Yan *et al*., 2019). A 0.1 mmol/L DPPH-ethanol solution was initially prepared. Different concentrations of DF suspension (0.5, 1, 1.5, 2.0, and 2.5 mg/mL) were then uniformly mixed with 3 mL of the DPPH-ethanol working solution and incubated for 30 min at 25°C in the dark. Subsequently, the absorbance of the resulting supernatant was measured at 517 nm using an ultraviolet spectrophotometer (MAPADA, Shanghai, China). A blank control group using 95% ethanol was employed. The DPPH clearance rate was calculated using the following formula:

$$\text{DPPH scavenging activity (\%)} = \left[\frac{A_{\text{blank}} - A_{\text{testing value}}}{A_{\text{blank}}}\right] \times 100 \quad (6)$$

The ABTS scavenging capacity of WBDF was evaluated according to the method of Díaz-Rubio with minor modifications (Díaz-Rubio *et al*., 2009). A DF suspension (2.5 mL) of varying concentrations (0.5, 1, 1.5, 2, and 2.5 mg/mL) was uniformly mixed with 2 mL of ABTS+ working solution and incubated for 6 min at room temperature in the dark. The absorbance of the resulting supernatant

was measured at 734 nm using an ultraviolet spectrophotometer (MAPADA, Shanghai, China), with deionized water used as the blank control. The ABTS scavenging rate was calculated using the following formula:

$$\text{ABTS scavenging activity}(\%) = \left[\frac{A_{blank} - A_{testing\ value}}{A_{blank}}\right] \times 100 \quad (7)$$

Experimental animal models and treatments

Modeling of slow transit constipation

Male Kunming mice aged 6–8 weeks were procured from the Hubei Province Center for Disease Control and Prevention. The mice were housed in an environment maintained at 25°C, with humidity ranging from 40% to 60%, and subjected to a 12-h light/dark cycle following a 1-week acclimatization period before experimentation. Modeling was conducted according to the method outlined by Wang with minor adjustments (Wang *et al*., 2023). The male Kunming mice were categorized into the following groups: control (saline), model (1.4 mg/mL loperamide hydrochloride solution), WB (1.4 mg/mL loperamide hydrochloride solution + WB), and extrusion modification of WB (1.4 mg/mL loperamide hydrochloride solution + extrusion modification of WB). The blank group received distilled water via gavage at a volume of 0.2 mL per 10 g of mouse body weight once a day for 8 consecutive days. Bran administration commenced on day 8, following loperamide hydrochloride gavage, with WB administered via gavage at a dosage of 0.5 g/kg for 7 consecutive days. Following the final administration, mice in each group were fasted except for water intake for 24 h. The administered dosage was 0.2 mL per 10 g of mouse body weight. Fecal water content, fecal count, first black-stool defecation time, and gastrointestinal transit rates were evaluated. The animal experimental protocol was approved by the Animal Research Committee of Hubei University of Chinese Medicine, and all procedures adhered to strict animal welfare guidelines in compliance with the European Community directives (EEC Directive of 1986; 86/609/EEC). The experiments were conducted in accordance with the ARRIVE guidelines, and the animal experimentation protocol approval number is HUCMS36047477.

Mouse defecation experiment

The time of initial defecation, the quantity/mass of defecated pellets, and the fecal water content were assessed as follows: mice were subjected to a 12-h fasting period, with access only to water, prior to the final administration. The blank group received saline via gavage, while the other groups received loperamide hydrochloride solution and the corresponding test substances. Following the administration of 0.2 mL of India ink via gavage for 30 min, all mice were returned to their normal water and food intake conditions and housed individually in cages. The time of the first appearance of the black stool was recorded upon completion of the gavage.

Within 6 h, feces were collected from the mice, the number of pellets was recorded, and the wet weight of the feces was measured. Subsequently, fecal samples were promptly collected and dried at 60°C until a constant weight was achieved. The dried weight of the mouse feces was then determined. The fecal water content was calculated using the following formula:

$$R = \frac{(W_1 - W_2)}{W_1} \times 100\% \quad (8)$$

where R represents the fecal water content, W_1 denotes the wet weight of feces (g), and W_3 signifies the dry weight of feces (g).

Propulsion rate determination of the intestine

The mice underwent a 12-h fasting period, with access only to water before the final administration. Following 30 min of gavage administration, all groups of mice received 0.2 mL of ink via gavage. Twenty minutes after the conclusion of the ink gavage, all mice were anesthetized and euthanized using the cervical dislocation method. The abdominal cavity was immediately opened, and the entire length of the intestines, from the pylorus to the anus, was extracted. The intestines were straightened without tension to obtain L1, representing the total length of the mouse intestine. The length of the ink within the intestines was measured as L2. The propulsion rate of the intestine was calculated using the following formula:

$$D = \frac{L_2}{L_1} \times 100\% \quad (9)$$

where D denotes the propulsion rate of the intestine, L_1 represents the total length of the mouse intestine (cm), and L_2 signifies the length of ink traveling within the intestine (cm).

Statistical analysis

The experiments were replicated three times. Data are presented as mean ± SD (n = 3). Analysis of variance was conducted to identify significant differences ($p < 0.05$) using Duncan's multiple-range test in SPSS 25.0 software (SPSS Inc., Chicago, IL, USA). Moreover, figures were generated using Origin 2022 software (Stat-Ease Inc., Minneapolis, MN, USA).

Results

Physicochemical properties

Effects of extrusion modification on WHC, OHC, and WSC of WBDF

Due to the abundant glucose residues in WBDF, which contain numerous hydrophilic groups, the DF exhibits strong water-absorbing and swelling properties. The WHC reflects the capacity of DF to absorb and retain water (Yang *et al*., 2021). Additionally, OHC is a key parameter in evaluating DF's ability to facilitate fat excretion and reduce serum cholesterol levels (Yang *et al*., 2011). The hypoglycemic and hypolipidemic effects of DFs are influenced by their chemical composition, structure, and physicochemical properties, particularly their hydration properties such as viscosity and water swelling capacity, as well as their adsorption capacity (Qi *et al*., 2016). The WHC, OHC, and WSC of both WBDF and E-WBDF are presented in Table 1. Compared to untreated WBDF, E-WBDF exhibited significantly increased WHC, OHC, and WSC ($p < 0.05$). These findings are consistent with those reported by Ma *et al.* (2023). The WHC increased by 1.57 g/g, representing a 17.06% increase, while the OHC increased by 2.26 g/g, marking a 26.49% increase. Similarly, the WSC increased by 1.17 mL/g, indicating an increase of 17.84%. The enhanced WHC and OHC may be attributed to the extrusion modification process, which compresses DFs into thin sheets, thereby increasing their surface area and loosening their internal structure to expose more hydrophilic groups, a conclusion supported by Yu et al. (2018). Additionally, the increased dissolution of WBDF particles in water results in swelling and expansion, contributing to the elevation of WSC, consistent with the findings of Ma *et al*. (2023).

Effects of extrusion modification on CAC and CSAC of WBDF

CAC serves as a crucial metric for evaluating the hypolipidemic efficacy of DFs. The present investigation focused on the adsorption of DF with cholesterol and glucose, factors believed to contribute to the hypolipidemic and hypoglycemic effects of DF (He *et al*., 2021). The CAC of E-WBDF surpassed that of WBDF under all conditions, registering 7.66 mg/g (pH = 7) and 18.56 mg/g (pH = 7). Generally, the CAC is influenced by the pH level of the environment. A comparison of CAC for the same sample under different pH conditions indicates that WBDF exhibits stronger CAC in neutral conditions (simulated small intestinal environment) than in acidic conditions (simulated gastric environment). This discrepancy can be attributed to the structural characteristics of cholesterol molecules, which possess a partial positive charge. In an acidic environment, the abundance of active hydrogen ions repels the cholesterol molecules, thereby diminishing their adsorption capacity (Li *et al*., 2022). The heightened cholesterol adsorption of E-WBDF compared to WBDF may be ascribed to structural changes induced by extrusion modification. Specifically, some IDF in WBDF underwent transformation into SDF, resulting in an increased proportion of SDF within WBDF. The binding capacity of SDF to sodium bile acids and cholesterol was notably higher than that of IDF (Luo *et al*., 2017). These findings align with those of previous researchers, who underscored that the increase in TDF and SDF could be linked to the degradation of cellulose, hemicelluloses, and lignin in WB (Long *et al*., 2014). These observations are consistent with the outcomes of thermogravimetric and XRD analyses.

Bile acids, produced in the liver and stored in the gallbladder, play a pivotal role in regulating cholesterol metabolism. DF possesses the ability to adsorb bile acids, offering several advantages. Primarily, it accelerates cholesterol breakdown in the body. Second, it hinders the absorption and utilization of fat, thereby preventing excessive fat intake. Moreover, by reducing the production of hypocholesterolemic acid, DF contributes to the protection and regulation of intestinal health (Taladrid *et al*., 2023). Additionally, DF traps sodium cholate in the small intestine, increasing the viscosity of gastrointestinal tract contents (Elleuch *et al*., 2011). In Figure 1B, significant variations in the adsorption capacity of WBDF for different concentrations of sodium cholate are evident. Within a specific range, as the concentration of sodium cholate increases, WBDF's adsorption capacity correspondingly increases. Conversely, it weakens at lower concentrations. Consequently, WBDF maintains dynamic equilibrium with sodium cholate in a neutral environment (simulated small intestine), facilitating normal fat metabolism in the intestine.

In comparison to WBDF, E-WBDF demonstrates significantly enhanced SCAC, likely due to its higher SDF content, WSC, and OHC (Table 1). DFs with elevated WSC and SDF content increase the medium's viscosity and form a network structure conducive to sodium cholate adsorption (Ma *et al*., 2016). At a sodium cholate

Table 1. WHC, OHC, and WSC of WBDF and E-WBDF.

	WHC (g/g)	OHC (g/g)	WSC (mL/g)
WBDF	7.34 ± 0.10[a]	6.27 ± 0.10[a]	5.39 ± 0.16[a]
E-WBDF	8.85 ± 0.25[b]	8.53 ± 0.78[b]	6.56 ± 0.28[b]

Data presented as means ± standard deviation (n = 3).
a, b: Values in the same column indicate significant differences ($p < 0.05$).
WHC: water-holding capacity, OHC: oil-holding capacity, WSC water swelling capacity, WBDF: wheat bran dietary fiber, E-WBDF: extrusion-modified wheat bran dietary fiber.

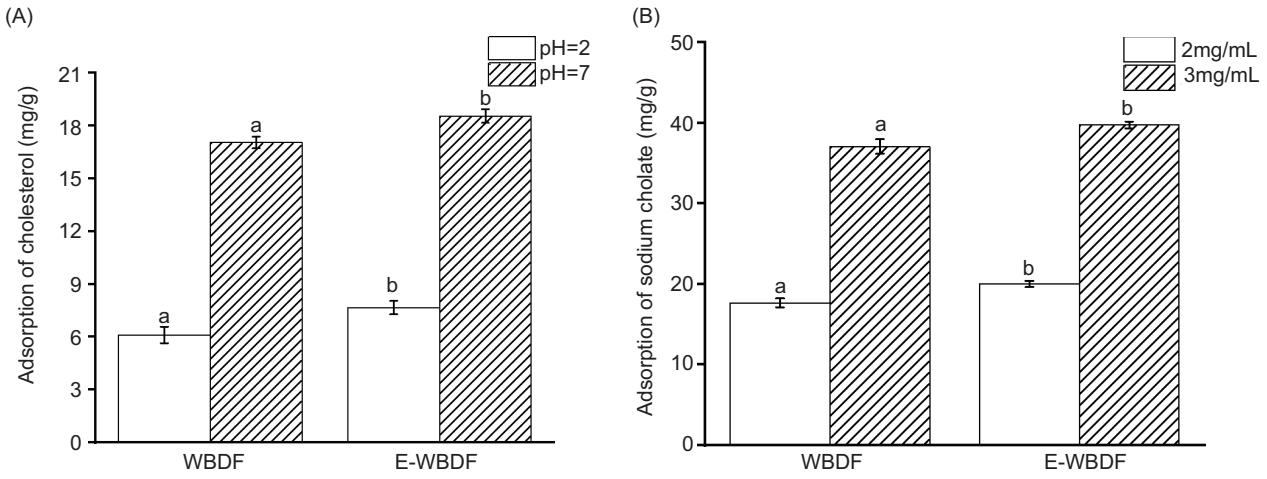

Figure 1. Cholesterol adsorption capacities CAC (A), and sodium cholate adsorption capacities SCAC (B) of WBDF and E-WBDF. The letters above the bars (a and b) represent the results of statistical analysis. Different letters indicate that the means are significantly different ($p < 0.05$) according to the t-test.

concentration of 2 mg/mL, E-WBDF's adsorption capacity is less affected, while at 3 mg/mL, it experiences an enhanced adsorption capacity, reaching a maximum of 39.76 mg/g. These findings align with those of previous researchers (Zheng *et al.*, 2021; Dong *et al.*, 2019).

Effects of extrusion modification on the thermal stability of WBDF

WBDFs treated with extrusion exhibited distinct thermal stabilities, as depicted in Figure 2. During the initial heating stage (0°C–250°C), all variants experienced a weight loss ranging from 3.83% to 5.52%, attributable to the evaporation of free water, loss of bound water, and volatile compounds. Notably, the chemical composition remained unaffected during this stage. Subsequently, between 250°C and 350°C, the curves exhibited a significant drop, indicating maximum weight loss attributed to the pyrolysis of hemicellulose and cellulose. Studies have indicated a carbon loss of approximately 60% within the temperature range of 220.85°C–407.7°C, attributed to cellulose and hemicelluloses (Zhang *et al.*, 2015). At temperatures exceeding 450°C, WBDF demonstrated a more pronounced decline and higher weight loss compared to E-WBDF, indicating that WBDF retains structural properties more similar to wheat DF samples. Therefore, it can be inferred that the thermal stability of E-WBDF is effectively enhanced within the range of 100°C to 300°C. Subsequent studies are expected to further validate this enhancement in thermal stability.

Effects of extrusion modification on the crystallinity of WBDF

As depicted in Figure 3, there were minor discrepancies in the positions of characteristic diffraction peaks observed at 15.8° and 21.5° (2θ) for the WBDFs. Following the extrusion treatment, the crystalline structure of the

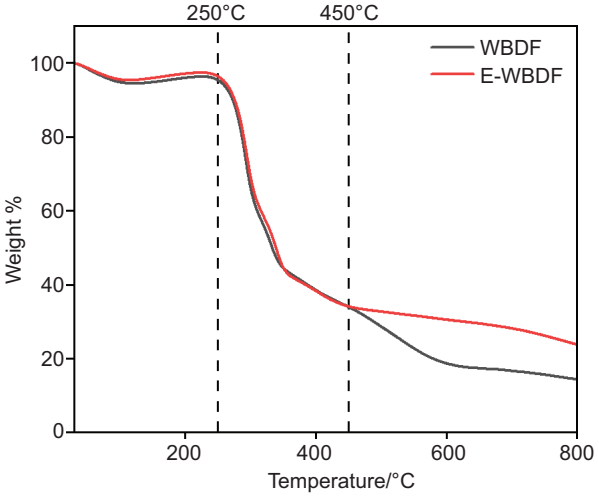

Figure 2. TGA profiles of WBDF and E-WBDF.

E-WBDF closely resembled that of WBDF, indicating that the structural crystallinity of E-WBDF remained unchanged. However, the peaks of E-WBDF appeared sharper, indicating an enhancement in its structural crystallinity. The calculated crystallinity of the DF and extrusion-modified samples was 16.35% and 17.69%, respectively, based on software curve fitting. This demonstrates an increase in crystallinity following extrusion modification compared to WBDF. The elevation in crystallinity could be attributed to the exposure of the DF's accessible edges. Research indicates that a higher degree of crystallinity enhances the capture and immobilization of interactions between molecules within the fiber, rendering it more stable. Consequently, an increase in crystallinity typically accompanies an increase in the thermal

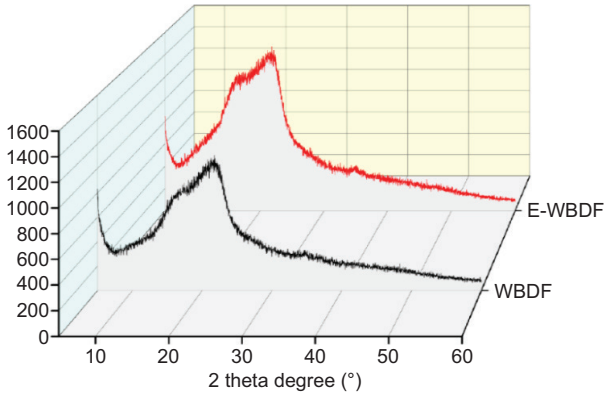

Figure 3. XRD pattern of WBDF and E-WBDF.

stability of fibers. These findings align with the outcomes of thermogravimetric analysis.

Effects of extrusion modification on function characteristics of WBDF

The antioxidant activity of WBDF and E-WBDF, encompassing DPPH and ABTS scavenging activities, is illustrated in Figure 4. As shown in Figure 4A, the DPPH scavenging capacity increased notably with increasing sample concentration before reaching a plateau, with E-WBDF exhibiting significantly greater activity compared to WBDF. Specifically, the DPPH scavenging ability surged within the sample concentration range of 0.5–1.0 mg/mL, with a subsequent slowdown observed as concentrations increased from 1.0 mg/mL to 2.5 mg/mL. After extrusion modification, the highest DPPH scavenging ability was observed at a sample concentration of 2.5 mg/mL, showcasing a 1.58-fold increase compared to the pre-modification scavenging capacity. This enhancement could be attributed to the release of more antioxidant substances, such as phenolic compounds found in WB, which effectively counteract oxidative stress, mitigating damage caused by reactive oxygen species to large biomolecules (Hu *et al*., 2018).

In Figure 4B, the impact of extrusion modification on ABTS scavenging capacity across concentrations ranging from 0.5 mg/mL to 2.5 mg/mL is depicted. The ABTS scavenging ability exhibited a pattern of rapid increase followed by stabilization as the sample concentration rose. Extrusion modification yielded the highest clearance rate of 70.01% at a sample concentration of 2.5 mg/mL.

Animal experiments

Effects of WBDF and E-WBDF on defecation in mice

In comparison to the control group, the model group exhibited an increase in the time taken for the first appearance of black feces by 66.25 min, a decrease in the number of fecal particles by 14.33 within 6 h, a reduction in total fecal output by 0.23 g over 6 h, and a decrease in fecal water content by 11.03%, as indicated in Table 2. These findings suggested the successful establishment of a constipation model in the mice. Relative to the model group, both the WBDF and E-WBDF groups showed a reduction in the time taken to pass the first black stool, along with an increase in the number of stool pellets, total stool output over 6 h, and fecal water content. The improvement was more pronounced in the E-WBDF group compared to the WBDF group, likely attributable to the higher content of SDF in the E-WBDF group. This higher SDF content facilitated an increase in fecal water content and modulation of intestinal motility, thereby promoting bowel movement. E-WBDF reduced the time taken to pass the first black feces by 20.83 min, increased the number of stools passed over 6 h by 2.66, raised the total stool output over 6 h by 0.06 g, and elevated fecal water content by 1.72% in mice compared to WBDF. Additionally, observation of fecal appearance and morphology revealed that feces in

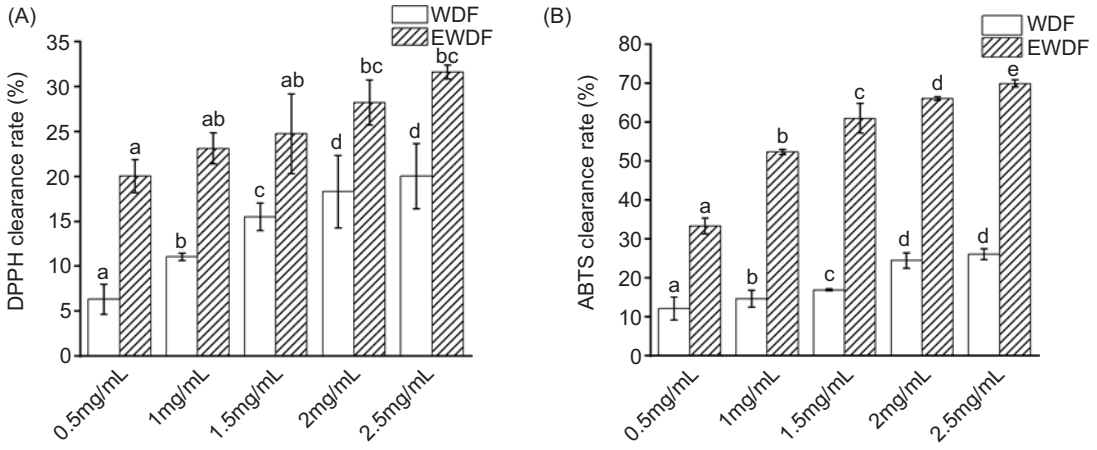

Figure 4. DPPH scavenging activity (A) and ABTS scavenging activity (B) of WBDF and E-WBDF.

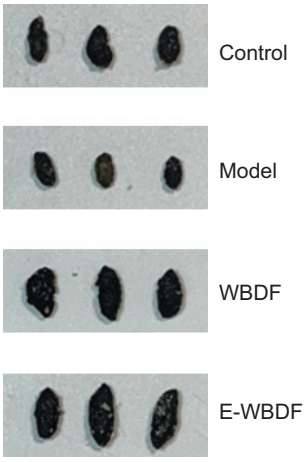

Figure 5. Effects of different test samples on fecal morphology in mice.

the E-WBDF group were notably larger, exhibited a moist surface, and had uniform coloration compared to the WBDF group, as depicted in Figure 5. This phenomenon may be attributed to the ability of DF to augment fecal water content, regulate intestinal motility, and facilitate defecation (Ge *et al*., 2016).

Effect of WBDF and E-WBDF on the propulsion rate of the small intestine in mice

As depicted in Table 3, the mouse small intestine propulsion experiment revealed that the ink propulsion rate was highest in the blank control group at 80.56%. In contrast, the model group exhibited a propulsion rate of 45%, which was 35.51% lower than that of the blank group. This decline indicated that the administration of loperamide hydrochloride via gavage weakened the peristaltic strength of the mice's small intestine, thereby successfully establishing the constipation model. The ink propulsion rates of both the WBDF and E-WBDF groups were 58.62% and 72.11%, respectively. These rates were higher than those of the model group, suggesting that the inclusion of WBDF could enhance intestinal peristalsis, with E-WBDF demonstrating a more pronounced effect. In Figure 6, the ink advancement distance was longest in the blank group and shortest in the model group, with the E-WBDF group exhibiting a greater ink advancement distance compared to the WBDF group. This difference can be attributed primarily to the ability of DF to promote peristalsis in the small intestine, consequently prolonging gastric emptying time. These findings align with those of previous studies (Zhang *et al*., 2018; Zhang *et al*., 2021).

Conclusions

The crystalline structure of E-WBDF closely resembled that of unmodified WBDF, with a slight improvement in crystalline strength, and TGA indicated enhanced thermal stability. E-WBDF also exhibited superior WHC, OHC, and WSC, along with higher CAC and SCAC

Table 2. Evaluation of time to the first appearance of black feces, number of feces in a 6-h period, quantification of fecal output in 6 h, and fecal water content in loperamide-induced constipation mice after treatment with different test samples.

Group	Time to the first appearance of black feces/min	Number of feces in 6 h	Quantification of fecal output during a 6-h period/g	Fecal water content/%
Control	146.25 ± 2.86^{a}	23.26 ± 4.19^{a}	0.38 ± 0.03^{c}	38.09 ± 2.56^{b}
Model	212.50 ± 11.06^{d}	9.33 ± 3.62^{c}	0.15 ± 0.02^{a}	27.06 ± 2.33^{a}
WBDF	183.33 ± 7.41^{c}	15.63 ± 2.27^{d}	0.25 ± 0.05^{b}	34.51 ± 1.62^{b}
E-WBDF	162.00 ± 6.38^{b}	18.33 ± 2.44^{b}	0.31 ± 0.01^{c}	36.23 ± 3.95^{b}

Data are presented as means ± standard deviation (n = 5).
a, b, c: Values in the same column indicate significant differences ($p < 0.05$).

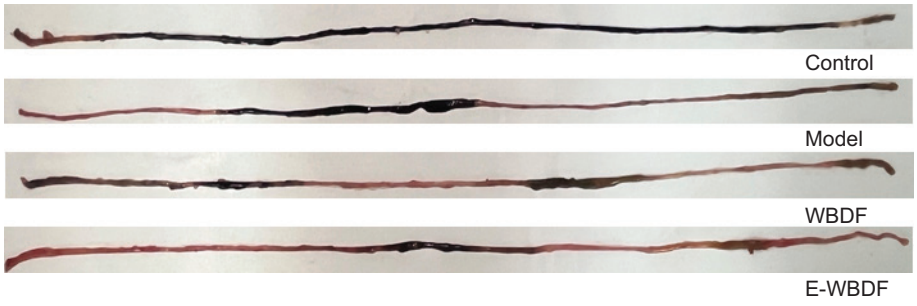

Figure 6. Influence of different test samples on small intestinal propulsion rate in mice.

Table 3. Total small intestine length, ink advancement distance, and intestinal transit rate in loperamide-induced constipation mice post-treatment.

Group	Total length of small intestine/cm	Ink advance distance	Propulsion rate/%
Control	45.25 ± 3.97[a]	36.20 ± 1.81[a]	80.37 ± 8.54[c]
Model	44.33 ± 4.17[a]	19.90 ± 1.22[c]	45.05 ± 1.86[a]
WBDF	42.67 ± 1.70[a]	25.00 ± 0.71[b]	58.62 ± 1.33[b]
E-WBDF	38.17 ± 2.95[a]	26.23 ± 1.23[b]	72.11 ± 6.78[c]

Data are presented as means ± standard deviation (n = 5).
a, b, c: Values in the same column indicate significant differences ($p < 0.05$).

compared to WBDF, providing a theoretical basis for subsequent mouse experiments. In the mouse trials, E-WBDF showed reduced time to pass the first black stool, fewer bowel pellets within 6 h, increased fecal water content, and an enhanced rate of ink propulsion, suggesting a more effective therapeutic outcome in alleviating constipation compared to WBDF. Consequently, E-WBDF, produced through extrusion modification, holds potential as a dietary supplement to improve intestinal health, with both theoretical and experimental foundations for addressing chronic or occasional constipation.

Declaration of Generative AI and AI-assisted Technologies in the Writing Process

The authors declare that there are no generative AI and AI-assisted technologies in the writing process**.**

Data Availability Statement

The data are available from the corresponding author upon suitable request.

Author Contributions

Z.W.: supervision, investigation, formal analysis; D.T.: writing–original draft, investigation; K.Z: resources, writing–review, and editing, data analysis; W.S.: writing–review and editing, X.J.: supervision, writing–review, and editing; B.L.: writing–review and editing.

Conflict of Interest

The authors declare no conflict of interest.

Funding

This work was supported by Hubei Province science and technology innovation program (2024BBB097), Special Project of Central Government Guiding Local Science and Technology Development of Hubei Province Development of Education (grant number 2020ZYYD015), and Project of Study on the effect of wheat bran on the quality of bread and its property changes during frozen storage (grant number 2020JYBQGDKFB15).

References

Barber, T.M., Kabisch, S., Pfeiffer, A.F.H., & Weickert, M.O. (2020). The health benefits of dietary fibre. Nutrients, 12, 3209. https://doi.org/10.3390/nu12103209

Bharucha, A.E. (2007). Constipation. Best Practice & Research Clinical Gastroenterology, 21(5), 709–731. https://doi.org/10.1016/j.bpg.2007.07.001

Brouns, F., van Rooy, G., Shewry, P., Rustgi, S., & Jonkers, D. (2019). Adverse reactions to wheat or wheat components. Comprehensive Reviews in Food Science and Food Safety, 18(6), 1437–1452. https://doi.org/10.1111/1541-4337.12475

Cao, J.H., Wang, K., Li, N.X., Zhang, L., Qin, L., He, Y., Wang, J., Qu, C., & Miao, J. (2023). Soluble dietary fiber and cellulose from Saccharina japonica by-product ameliorate loperamide-induced constipation via modulating enteric neurotransmitters, short-chain fatty acids and gut microbiota. International Journal of Biological Macromolecules, 226, 1319–1331. https://doi.org/10.1016/j.ijbiomac.2022.11.243

Cheng, W., Sun, Y.J., Fan, M.C., Li, Y., Wang, L., & Qian, H.F. (2022). Wheat bran, as the resource of dietary fiber: a review. Critical Reviews in Food Science and Nutrition, 62, 7269–7281. https://doi.org/10.1080/10408398.2021.1913399

DeVries, J.W. (2003). On defining dietary fibre. Proceedings of the Nutrition Society, 62, 37–43. https://doi.org/10.1079/PNS2002234

Díaz-Rubio, M.E., Pérez-Jiménez, J., & Saura-Calixto, F. (2009). Dietary fiber and antioxidant capacity in Fucus vesiculosus products. International Journal of Food Science and Nutrition, 60(Suppl. 23–34. https://doi.org/10.1080/09637480802189643

Dong, J.L., Wang, L., Lü, J., Zhu, Y.Y., & Shen, R.L. (2019). Structural, antioxidant and adsorption properties of dietary fiber from foxtail millet (Setaria italica) bran. Journal of the Science of Food and Agriculture, 99, 3886–3894. https://doi.org/10.1002/jsfa.9611

Elleuch, M., Bedigian, D., Roiseux, O., Besbes, S., Blecker, C., & Attia, H. (2011). Dietary fibre and fibre-rich by-products of food processing: characterisation, technological functionality and commercial applications: a review. Food Chemistry, 124, 411–421. https://doi.org/10.1016/j.foodchem.2010.06.077

Ge, X. L., Tian, H. L., Ding, C., Gu, L., Wei, Y., Gong, J., Zhu, W., Li, N., & Li, J. (2016). Fecal microbiota transplantation in combination with soluble dietary fiber for treatment of slow transit

constipation: a pilot study. Archives of Medical Research, 47, 236–242. https://doi.org/10.1016/j.arcmed.2016.06.005

He, Y., Wang, B., Wen, L., Wang, F., Yu, H., Chen, D., Su, X., & Zhang, C. (2022). Effects of dietary fiber on human health. Food Science & Human Wellness, 11, 1–10. https://doi.org/10.1016/j.fshw.2021.07.001

Hu, Y., Wang, L., & Li, Z. (2018). Superheated steam treatment on wheat bran: enzymes inactivation and nutritional attributes retention. LWT, 91, 446–452. https://doi.org/10.1016/j.lwt.2018.01.086

Kahlon, T. S., Smith, G. E., & Shao, Q. (2005). In vitro binding of bile acids by kidney bean (Phaseolus vulgaris), black gram (Vigna mungo), bengal gram (Cicer arietinum) and moth bean (Phaseolus aconitifolins). Food Chemistry, 90, 241–246. https://doi.org/10.1016/j.foodchem.2004.03.046

Lai, H., Li, Y., He, Y., Chen, F., Mi, B., Li, J., Xie, J., Ma, G., et al. (2023). Effects of dietary fibers or probiotics on functional constipation symptoms and roles of gut microbiota: a double-blinded randomized placebo trial. Gut Microbes, 15, 2197837. https://doi.org/10.1080/19490976.2023.2197837

Li, M.X., Liu, Y.X., Yang, G., Sun, L., Song, X., Chen, Q., Bao, Y., Luo, T., & Wang, J. (2022). Microstructure, physicochemical properties, and adsorption capacity of deoiled red raspberry pomace and its total dietary fiber. LWT, 153, 112478. https://doi.org/10.1016/j.lwt.2021.112478

Liu, X., Suo, K.K., Wang, P., Li, X., Hao, L., Zhu, J., Yi, J., Kang, Q., Huang, J., & Lu, J. (2021). Modification of wheat bran insoluble and soluble dietary fibers with snail enzyme. Food Science and Human Wellness, 10, 356–361. https://doi.org/10.1016/j.fshw.2021.02.027

Long, D., Ye, F., & Zhao, G. (2014). Optimization and characterization of wheat bran modified by in situ enhanced CO_2 blasting extrusion. LWT – Food Science and Technology, 59, 605–611. https://doi.org/10.1016/j.lwt.2014.07.017

Luo, X., Wang, Q., Zheng, B., Lin, L., Chen, B., Zheng, Y., & Xiao, J. (2017). Hydration properties and binding capacities of dietary fibers from bamboo shoot shell and its hypolipidemic effects in mice. Food and Chemical Toxicology, 109, 1003–1009. https://doi.org/10.1016/j.fct.2017.02.029

Ma, M.M., & Mu, T.H. (2016). Effects of extraction methods and particle size distribution on the structural, physicochemical, and functional properties of dietary fiber from deoiled cumin. Food Chemistry, 194, 237–246. https://doi.org/10.1016/j.foodchem.2015.07.095

Ma, Q., Yu, Y., Zhou, Z., Wang, L., & Cao, R. (2023). Effects of different treatments on composition, physicochemical and biological properties of soluble dietary fiber in buckwheat bran. Food Bioscience, 53, 102517. https://doi.org/10.1016/j.fbio.2023.102517

Maffei, H.V.L., & Vicentini, A.P. (2011). Prospective evaluation of dietary treatment in childhood constipation: high dietary fiber and wheat bran intake are associated with constipation amelioration. Journal of Pediatric Gastroenterology and Nutrition, 52(1), 55–59. https://doi.org/10.1097/MPG.0b013e3181e2c6e2

Nawrocka, A., Szymańska-Chargot, M., Miś, A., Wilczewska, A.Z., & Markiewicz, K.H. (2017). Aggregation of gluten proteins in model dough after fibre polysaccharide addition. Food Chemistry, 231, 51–60. https://doi.org/10.1016/j.foodchem.2017.03.117

Oh, H., Kim, H., Lee, D.H., Lee, A., Giovannucci, E.L., Kang, S.S., & Keum, N. (2019). Different dietary fibre sources and risks of colorectal cancer and adenoma: a dose–response meta-analysis of prospective studies. British Journal of Nutrition, 122(6), 605–615. https://doi.org/10.1017/S0007114519001454

Orozco-Angelino, X., Espinosa-Ramírez, J., & Serna-Saldívar, S.O. (2023). Extrusion as a tool to enhance the nutritional and bioactive potential of cereal and legume by-products. Food Research International, 169, 112889. https://doi.org/10.1016/j.foodres.2023.112889

Prückler, M., Siebenhandl-Ehn, S., Apprich, S., Höltinger, S., Haas, C., Schmid, E., & Kneifel, W. (2014). Wheat bran-based biorefinery 1: Composition of wheat bran and strategies of functionalization. LWT – Food Science and Technology, 56, 211–221. https://doi.org/10.1016/j.lwt.2013.12.004.

Qi, J., Li, Y., Masamba, K.G., Shoemaker, C.F., Zhong, F., Majeed, H., & Ma, J. (2016). The effect of chemical treatment on the in vitro hypoglycemic properties of rice bran insoluble dietary fiber. Food Hydrocolloids, 52, 699–706. https://doi.org/10.1016/j.foodhyd.2015.08.008

Ramos-Enríquez, J.R., Ramírez-Wong, B., Robles-Sánchez, R.M., Robles-Zepeda, R.E., González-Aguilar, G.A., & Gutiérrez-Dorado, R. (2018). Effect of extrusion conditions and the optimization of phenolic compound content and antioxidant activity of wheat bran using response surface methodology. Plant Foods for Human Nutrition, 73(3), 228–234. https://doi.org/10.1007/s11130-018-0679-9

Sangnark, A., & Noomhorm, A. (2003). Effect of particle sizes on functional properties of dietary fibre prepared from sugarcane bagasse. Food Chemistry, 80(2), 221–229. https://doi.org/10.1016/S0308-8146(02)00257-1

Segal, L., Creely, J.J., Martin, A.E., & Conrad, C.M. (1959). An empirical method for estimating the degree of crystallinity of native cellulose using the X-ray diffractometer. Textile Research Journal, 29(10), 786–794. https://doi.org/10.1177/004051755902901003

Solah, V.A., Kerr, D.A., Hunt, W.J., Johnson, S.K., Boushey, C.J., Delp, E.J., Meng, X., Gahler, R.J., James, A.P., Mukhtar, A.S., Fenton, H.K., & Wood, S. (2017). Effect of fibre supplementation on body weight and composition, frequency of eating and dietary choice in overweight individuals. Nutrients, 9, 149. https://doi.org/10.3390/nu9020149

Sui, W.J., Xie, X., Liu, R., Wu, T., & Zhang, M. (2018). Effect of wheat bran modification by steam explosion on structural characteristics and rheological properties of wheat flour dough. Food Hydrocolloids, 84, 571–580. https://doi.org/10.1016/j.foodhyd.2018.06.027

Taladrid, D., Rebollo-Hernanz, M., Martin-Cabrejas, M.A., Moreno-Arribas, M.V., & Bartolomé, B. (2023). Grape pomace as a cardiometabolic health-promoting ingredient: activity in the intestinal environment. Antioxidants (Basel), 12, 979. https://doi.org/10.3390/antiox12040979

Threapleton, D.E., Greenwood, D.C., Evans, C.E.L., Cleghorn, C.L., Nykjaer, C., Woodhead, C., Cade, J.E., Gale, C.P., & Burley, V.J.

(2013). Dietary fibre intake and risk of cardiovascular disease: systematic review and meta-analysis. BMJ, 347, f6879. https://doi.org/10.1136/bmj.f6879

Wang, L., Xie, S., Jiang, X., Xu, C., Wang, Y., Feng, J., & Yang, B. (2023). Therapeutic effects of Bombax ceiba flower aqueous extracts against loperamide-induced constipation in mice. Pharmaceutical Biology, 61, 125–134. https://doi.org/10.1080/13880209.2022.2157841

Wang, T., Sun, X., Zhou, Z., & Chen, G. (2012). Effects of microfluidization process on physicochemical properties of wheat bran. Food Research International, 48(2), 742–747. https://doi.org/10.1016/j.foodres.2012.06.015

Yan, J., Hu, J., Yang, R., & Zhao, W. (2018). A new nanofibrillated and hydrophobic grafted dietary fibre derived from bamboo leaves: enhanced physicochemical properties and real adsorption capacity of oil. International Journal of Food Science & Technology, 53(10), 2394–2404. https://doi.org/10.1111/ijfs.13832

Ye, G.D., Wu, Y.N., Wang, L.P., Tan, B., Shen, W., Li, X., Liu, Y., Tian, X., & Zhang, D. (2021). Comparison of six modification methods on the chemical composition, functional properties and antioxidant capacity of wheat bran. LWT, 149, 111996. https://doi.org/10.1016/j.lwt.2021.111996

Yu, G., Bei, J., Zhao, J., Li, Q., & Cheng, C. (2018). Modification of carrot (Daucus carota Linn. var. sativa Hoffm.) pomace insoluble dietary fiber with complex enzyme method, ultrafine comminution, and high hydrostatic pressure. Food Chemistry, 257, 333–340. https://doi.org/10.1016/j.foodchem.2018.03.037

Zhang, J., Choi, Y.S., Yoo, C.G., Kim, T.H., Brown, R.C., & Shanks, B.H. (2015). Cellulose-hemicellulose and cellulose-lignin interactions during fast pyrolysis. ACS Sustainable Chemistry & Engineering, 3(2), 293–301. https://doi.org/10.1021/sc500664h

Zhang, S., Jia, X., Xu, L., Xue, Y., Pan, Q., Shen, W., & Wang, Z. (2022). Effect of extrusion and semi-solid enzymatic hydrolysis modifications on the quality of wheat bran and steamed bread containing bran. Journal of Cereal Science, 108, 103577. https://doi.org/10.1016/j.jcs.2022.103577

Zhang, X.Y., Tian, H.L., Gu, L.L., Nie, Y., Ding, C., Ge, X., Yang, B., Gong, J., & Li, N. (2018). Long-term follow-up of the effects of fecal microbiota transplantation in combination with soluble dietary fiber as a therapeutic regimen in slow transit constipation. Science China Life Sciences, 61(6), 779–786. https://doi.org/10.1007/s11427-017-9229-1

Zheng, Y.J., Wang, X.Y., Tian, H.L., Li, Y., Shi, P.Q., Guo, W.Y., & Zhu, Q.Q. (2021). Effect of four modification methods on adsorption capacities and in vitro hypoglycemic properties of millet bran dietary fibre. Food Research International, 147, 110565. https://doi.org/10.1016/j.foodres.2021.110565